FIBER-OPTIC SYSTEM FOR CONTROL OF THE ORIENTATION OF OBJECTS IN SPACE

Oleksandr S. Hnatenko[a], Yuriy P. Machekhin[a], Victor Bilichenko[b], Valeriy I. Zarytskyi[a] Yaroslav Yaroslavskyy[c,d], Jacek Klimek*[e] Kanat Mussabekov[f], Bakhyt Yeraliyeva[g], Ainur Ormanbekova[h]
[a]Kharkiv National University of Radio Electronics, 14 Nauku Ave., Kharkiv, Ukraine, [b]Vinnytsia National Technical University, [c]National University Odessa Polytechnic, [d]Vinnytsia Scientific and Research and the Design Institute of Land Management, [e] Lublin University of Technology, Nadbystrzycka 38 D, 20 – 618 Lublin, [f]Academy of Logistics and Transport, Almaty, Kazakhstan, [g]M.Kh.Dulaty Taraz Regional University, Taraz, Kazakhstan, [h]Al-Farabi Kazakh National University, Almaty, Kazakhstan

ABSTRACT

This article illustrates a system for stabilizing objects in space based on integral fiber elements. The proposed system showed results commensurate with similar systems with a length of tens of kilometers of SMF-28 optical fiber, while using PANDA type optical fiber is only 200 m. In the work, a model of the system was developed and experimental studies of the response and angular velocity of the gyroscope were carried out.

Keywords: optical fiber, Sagnac interferometer, laser, polarization, gyroscope, optics, photonics.

1. INTRODUCTION

Modern optical information and control inertial navigation systems (INS) should autonomously determine many physical parameters[1-3]. The location (course) of an object in the inertial coordinate system (CS): its speed, acceleration and other parameters necessary to control the movement and determine its location in space are really important. To obtain information about the movement of an object, its INS, first of all, includes: gyroscopes for determining the angles of inclination of the main axes in the inertial CS and accelerometers for determining linear accelerations[3-6]. Depending on the design of a closed optical loop (interferometer), optical gyroscope (OG) are divided into ring laser gyroscopes (RLG), fiber optical gyroscopes (FOG) of the interferometric type (IFOG - Interferometric Fiber Optic Gyroscope) and FOG with a passive resonator (RFOG − Resonant Fiber Optic Gyroscope). FOG of the interferometric type is a Sagnac interferometer, in which a circular optical circuit is replaced by a sensitive coil of a large number of turns of optical fiber (OF) to achieve the required level of FOG sensitivity (the length of the FOG can reach several kilometers[8,9]. In a single-mode OF, the propagation of two independent modes with orthogonal polarization is possible. But since the optical fibers do not have a completely constant axial symmetry, the phase constant modes are different. Between two modes with different polarizations, there is a constant energy exchange, the characteristics of which change under external influence, so the light in the OF usually has circular polarization with unstable parameters. All this leads to the drift of the output signal. Thus, the optical circuit of the FOG requires the construction of a onemode OF with the preservation of the polarization position and minimal loss, which significantly increases the budget segment of such FOGs. Therefore, the relevance of the work lies in the need to develop the theory and practice of FOG of interferometric and resonant types using a PANDA optical fiber coil as a sensitive element[21,22].

*j.klimek@pollub.pl

Optical Fibers and Their Applications 2023, edited by Waldemar Wójcik, Zbigniew Omiotek, Andrzej Smolarz, Proc. of SPIE Vol. 12985, 1298508 · © 2023 SPIE
0277-786X · doi: 10.1117/12.3023026

2. THEORETICAL FOUNDATIONS

M. Sagnac's experience is based on the use of an optical interferometer. The principle of operation of the interferometer is as follows: a beam of electromagnetic (EM) radiation is divided in the volume of the interferometer by means of a device into two or more coherent beams. Each of these beams passes through different optical paths and is directed to the screen, creating an interference pattern on it, which can be used to determine the phase difference of the interfering beams. M. Sagnac's experiments showed that the interference pattern shifts as the interferometer rotates, and the shift is proportional to the rotation speed. Consider the propagation of two light beams in a flat closed circular contour of radius R (Figure 1)[10,11,12.]

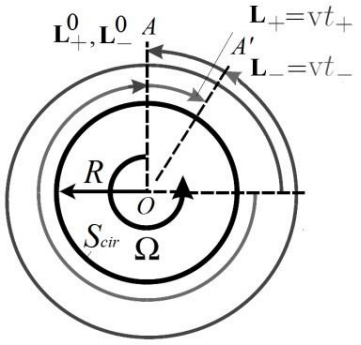

Figure 1. Influence of the rotation speed of the interferometer on the time of passage of light rays

The contour area is perpendicular to the axis of rotation passing through the center of the circle O. In a fixed interferometer, the round trip time t0 along the contour will be the same for both beams [10,11,12].

$$t_0 = \frac{L_0}{c} = \frac{2\pi R}{c}, \tag{1}$$

where c is the speed of light.

When the interferometer rotates during the round trip, point A will move to point A', so the propagation conditions for colliding beams will become unequal. Optical path, passing beam propagating in the direction of rotation[13,19].

$$L_+ = 2\pi R + \Omega R t_0, \tag{2}$$

and the path passing the beam in the opposite rotation direction will now be

$$L_- = 2\pi R - \Omega R t_0, \tag{3}$$

where Ω – angular speed of rotation.

Substituting the value t_0 and taking into account that the speed of propagation of electromagnetic wave beams, in accordance with Einstein's theory[10,11,12].

$$: t_\pm = \frac{L_\pm}{c} = t_0 \pm \frac{2\pi R^2}{c^2}\Omega. \tag{4}$$

That is, the difference in the round-trip time of the colliding beams:

$$\Delta t = \frac{4\pi R^2}{c^2}\Omega, \tag{5}$$

is proportional to the rotation speed Ω.

Taking into account the difference in the round-trip time of the contour by the colliding beams, we can obtain the difference in the optical path lengths when the light beams propagate in opposite directions:

$$\Delta L = c\Delta t = \frac{4\pi R^2}{c}\Omega. \quad (6)$$

The presence of a difference in optical paths during the propagation of light beams in opposite directions leads to a shift in the interference pattern. It should be noted that the expression for ΔL was obtained for an observer in a fixed frame of reference. In the general case, the physical picture must be considered from the point of view of the general theory of relativity. According to this theory, clocks that rotate on a turntable are out of sync with clocks that are in an inertial frame of reference[14,15,16]. This difference leads to different round trip times of the closed circuit by counterpropagating light beams. For an electromagnetic wave, its frequency f (λ=c/f - wavelength) and period T, that is, the time required to change the phase by 2π, are determined, which are interconnected as T=1/f. Accordingly, the phase change (phase shift) $\Delta\phi$ over time Δt will be

$$\Delta\phi = 2\pi\frac{\Delta t}{T} = 2\pi f\Delta t = \omega\Delta t\,, \quad (7)$$

where ω is the cyclic or angular frequency.

After substituting Δt into (7), the phase shift will look like this

$$\Delta\varphi = \frac{8\pi^2 R^2 f}{c^2}\Omega = \frac{4\varpi S_{cir}}{c^2}\Omega = \frac{4kS_{cir}}{c}\Omega = \frac{8\pi S_{cir}}{\lambda c}\Omega\,, \quad (8)$$

where $S_{cir} = \pi R^2$ – the area of the round interferometer with radius *R*, $k=2\pi/\lambda$ is the wavenumber. The form of relations (8) is a generalization of the analytical description of the Sagnac effect, which does not depend on the shape of the optical path, the position of the center of rotation, and the refractive index. The use of a multi-turn coil makes it possible to increase the Sagnac effect in proportion to the length of the optical fiber (the number of turns in the coil), practically without changing the dimensions of the device. So, the phase difference of counter propagating waves $\Delta\phi$ in a multi-turn circuit can be determined using several more equivalent formulas[15,16,17].

$$\Delta\phi = \frac{2L^2}{\lambda cN}\Omega, \quad (9)$$

where $s = \pi R_2$ is the area of one turn, *N* is the number of turns, *R* is the turn radius, $L = 2\pi RN$ is the total length of the multi-turn coil. The dimensions of such a gyroscope are determined mainly by the diameter of the coil (*2R*) and height. The latter, in turn, depends on the length of the optical fiber and the diameter of its outer cladding (~200 μm), on the number of turns and layers during winding, and, as a rule, is much smaller than the diameter. Comparison of expressions (1), (2) and (9) shows that in a single-turn circuit (N = 1) the sensitivity increases as the square of the total length of the optical fiber, and in a multi-turn circuit it increases proportionally to the total length [12,13,18].

3. STRUCTURAL DIAGRAM AND DESIGN OF THE FOG

The Sagnac fiber interferometer acts as the main element of a fiber-optic gyroscope. The principle of FOG operation is based on the Sagnac effect, according to which a phase shift of counterpropagating electromagnetic waves occurs in a ring interferometer, which will have an angular velocity. A quartz single-mode optical fiber is used as a waveguide in the FOG. A fiber 200 meters long is wound on a reel. In order to accurately and accurately determine the angular velocity based on the measured value of the phase difference of the oncoming waves, it is necessary to exclude possible additive and multiplicative effects of negative physical impacts. Negative effects are also associated with the processes of scattering and reflection of light along the optical path, the effect of polarization nonreciprocity, etc.[14-19].To solve the problem caused by the shortcomings of quartz fiber, we propose a Panda-type optical fiber as a FOG waveguide; the scheme of the developed fiber-optic gyroscope is shown in Fig. 2.

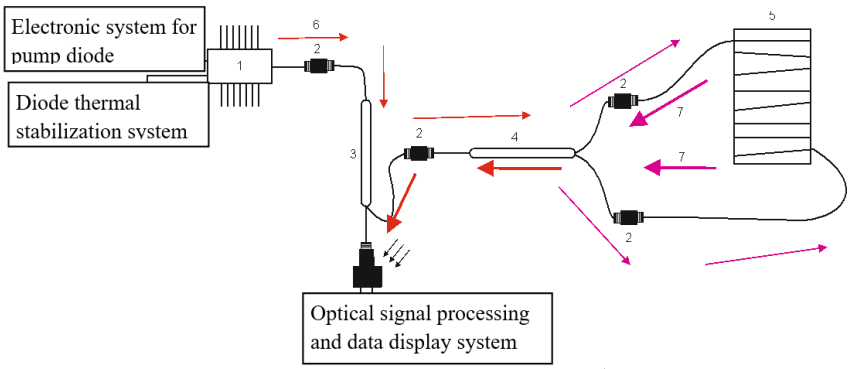

Figure 2. Scheme of FOG: 1 - laser superluminescent diode; 2 - coupling for connecting fiber-integrated elements; 3 - circulator; 4 – splitter/combiner; 5 - coil with optical fiber; 6 – direction of radiation from the laser diode; 7 - direction of radiation after passing through the coil with fiber; 8 - photodiode

Figure 3 shows the layout of the developed gyroscope.

Figure 3. Layout of the developed gyroscope

4. ELECTRONIC SYSTEMS FOR FOG

The electrical part of the gyroscope consists of two boards: a power board and data digitization. Board projects consist of: electrical circuit diagrams; printed circuit board design; list of elements; component libraries. The design of the electrical circuit and printed circuit board was made in Altium Designerversion 16. For the operation of the gyroscope, software was written in C language in the STM32CubeIDE 1.6.1 development environment. Description of the power board (power board). In general, the board is shown in Figure 4. Power (12 V) is supplied to connector P11 or P12. On the transistor VT16, protection is provided against supplying the wrong polarity of the supply voltage. To increase the sensitivity of the device, thermal stabilization of the laser diode crystal was performed with an accuracy of ±0.2 °C. This implementation of thermal stabilization allows heating and cooling the laser diode crystal. The thermal stabilization system maintains the temperature of the crystal at 25°C.

In the process of creating and debugging the software, five modes of operation of the laser diode were implemented: in the first mode, a constant current through the laser diode is maintained at the level of 100 mA; in the second mode, a constant current through the laser diode is maintained at the level of 200 mA; in other operating modes, the current through the laser diode is modulated in the form of a sinusoid.

After power is applied, thermal stabilization is activated regardless of the selected mode. The device has protection against overvoltage or undervoltage. If the supply voltage is less than 9.5 V or more than 14.5 V, the device goes into protective mode, turning off thermal stabilization and laser diode radiation. When the supply voltage returns to the recommended range, the device starts working again. In the final version of the software, the first operating mode is

turned on automatically, while the source code retains the ability to manually select the operating mode using the buttons, if necessary, you can disable the autostart of the first mode.

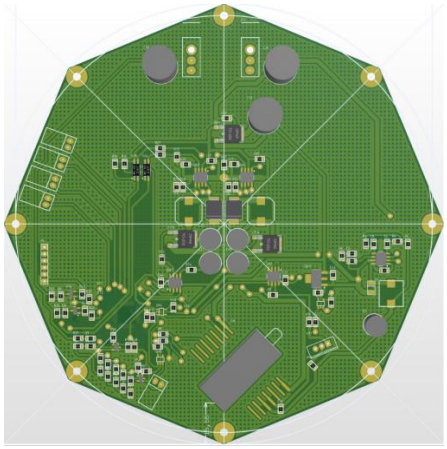

Figure 4. Diode power and control board

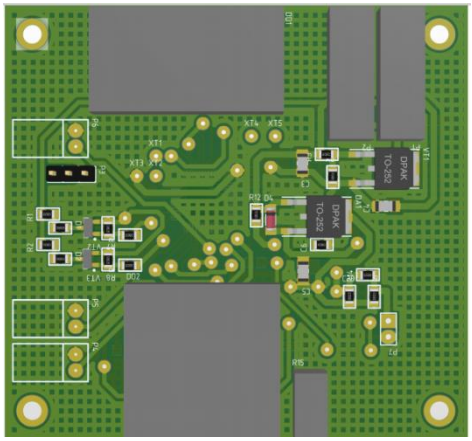

Figure 5. General view of the data digitization board

To reduce noise in the power supply current of the laser diode, a hybrid power supply circuit was used. First, the voltage is lowered on the pulse converter, and then the analog current stabilization of the laser diode takes place. The software of the power board implements the ability to select the current and, accordingly, the radiation power of the laser LED. The laser LED current is selected by setting the reference voltage at the output of the DAC (digital-to-analog converter) of the microcontroller. Initialization of the DAC is performed using the code written in C language.

To stabilize the operating characteristics of the radiation of a laser LED, thermal stabilization of its internal crystal was used. The temperature of the laser LED crystal is estimated using the ADC (analogue digital converter) of the microcontroller. ADC initialization is performed using code written in C language. Temperature control is carried out by generating PWM (pulse width modulation) timer control signals. To calculate the required PWM value of the timer signals based on the current temperature of the laser LED crystal, a PID (proportional-integral-derivative) controller is used. The software of the power board also implements control of the supply voltage of the gyroscope; if the tolerances are exceeded, an emergency shutdown of the laser diode occurs for its (diode) safety

Data processing board (digitization board). To receive optical signals, an ingaas-120l-fc photodiode is used, then the signal is fed to the DA3 operational amplifier and then the amplified signal is digitized by the DD4 microcontroller. An L3GD20 digital gyroscope chip was used to determine the direction of rotation. To transmit data over the air (radiation level at the input and direction of rotation) to an external device (computer), a radio module on the NRF24L01 chip was used for analysis. The transmission of information and rotation is transmitted via the RS232 interface.

5. RESULTS

The software of the data processing board implements signal processing from the photodiode. The ADC reads the voltage at the photodiode and filters the values. To determine the direction of rotation, a digital gyroscope based on the L3GD20 chip was used. After processing the data from the photodiode and determining the direction of rotation, the data is prepared and sent by radio to the data processing receiving board. The radio channel between the data processing board and the processed data receiving board is implemented on the basis of NRF24L01 microcircuits. The use of a radio channel made it possible to use the stand. A device for rotation and evaluation of the stability of readings at different rotation speeds for a long time was fixed on the stand. After carrying out experiments and measurements, data were obtained, Fig.6. This figure shows two graphs. The upper graph shows the change in voltage at the receiving photodiode as the gyroscope rotates in space. Voltage peaks correspond to the speed of rotation of the gyroscope in space. The lower graph shows the change in the value of the direction of rotation data. Initially, the value was 15 (corresponding to 0x0F

- the direction of rotation is not defined), during the rotation, the value changed to 61 (corresponding to 0x3D - clockwise rotation).

Preliminary studies of a fiber gyroscope prototype were carried out and the angular velocity was determined, corresponding to - + -300 (deg / s). Figure 7 shows the experimental dependence of the gyroscope response to the angular velocity.

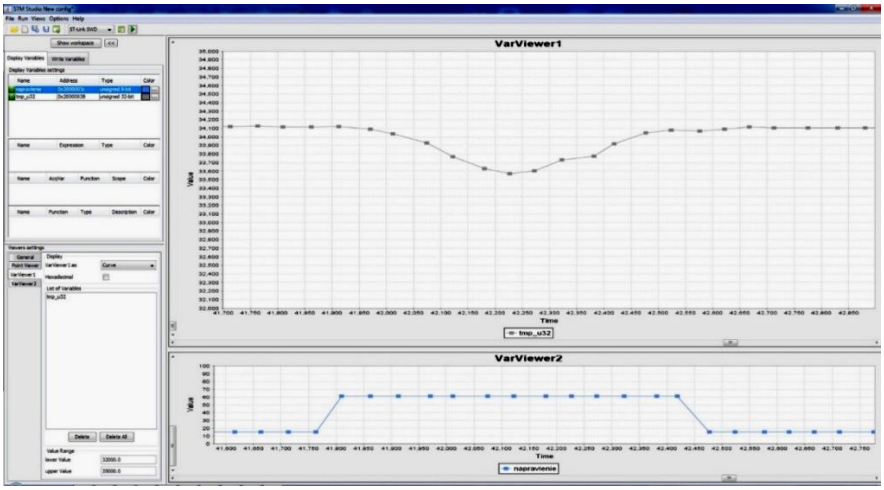

Figure 6. Photo of data processing of the device operation

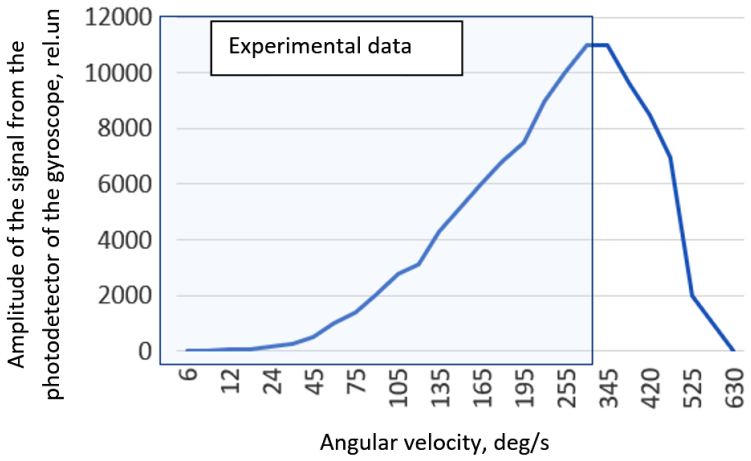

Figure 7. Dependence of the photodiode signal amplitude on the angular velocity of the system rotation

6. CONCLUSIONS

The design of a fiber-optic gyroscope has been developed in this work. The design was based on an optical fiber with polarization support, which made it possible to obtain interference and phase difference with an optical fiber length of 200 m. Since when using an SMF-28 optical fiber, its length should be several kilometers, this is due to the unstable polarization orientation in these types of optical fibers.

When using an optical fiber with a stable polarization orientation at a length of 200 m, it was possible to detect the angular velocity of the object's rotation at a maximum of +-300 deg/s. This is not the most sensitive device of this type, but an increase in the length of the optical fiber to 500 m will increase the sensitivity of the sensor by 1.8 times. The results of this work contribute to the development of fiber-optic gyroscopes using specific optical fibers, including photonic crystal fibers.

REFERENCES

[1] Tolegenova, A., Kisała, P., Zhetpisbayeva, A., Mamyrbayev, O., Medetov, B., " Experimental determination of the characteristics of a transmission spectrum of tilted fiber Bragg gratings," Metrology and Measurement Systems 26(3), 581–589, (2019).

[2] Kisała, P., "Physical foundations determining spectral characteristics measured in Bragg gratings subjected to bending," Metrology and Measurement Systems 29(3), 573–584, (2022).

[3] Kisała, P., Kalizhanova, A., 3), Kozbakova, A., Yeraliyeva, B., "Identification of cladding modes in SMF-28 fibers with TFBG structures," Metrology and Measurement Systems 30(3), 507–518, (2023).

[4] Léfevre, H. C., Steib, A., Claire, A., Sekeriyan, A., Couderette, A., Pointel, A. L., Viltard, A., Bonnet, A., Frénois, A., Gandoin, A., et al. "The fiber optic gyro 'adventure' at Photonetics, iXsea and now iXblue. In Proceedings of the Optical Waveguide and Laser Sensors," International Society for Optics and Photonics: Bellingham, WA, USA, 11405, 1140505 (2020).

[5] Song, N., Xu, X., Zhang, Z., Gao, F., Wang, X. "Advanced Interferometric Fiber Optic Gyroscope for Inertial Sensing: A Review," Journal of Lightwave Technology, 41(13), 1–14 (2023).

[6] Lefevre, H. C., "The Fiber-Optic Gyroscope," Artech House: Norfolk County, MA, USA, (2022).

[7] Schmelzbach, C., Donner, S., Igel, H., Sollberger, D., Taufiqurrahman, T., Bernauer, F., Häusler, M., Renterghem, C.V., Wassermann, J., Robertsson, J. "Advances in 6C seismology: Applications of combined translational and rotational motion measurements in global and exploration seismology," Geophysics, 83, WC53–WC69, (2018).

[8] Guattari, F., Moluçon, C., Bigueur, A., Ducloux, E., de Toldi, E., Honthaas, J., Lefèvre, H., "Touching the limit of FOG angular random walk: Challenges and applications," In Proceedings of the 2016 DGON Intertial Sensors and Systems (ISS), Karlsruhe, Germany, 1–13 (2016).

[9] Shin, S., Sharma, U., Tu, H., Jung, W., Boppart, S.A., "Characterization and Analysis of Relative Intensity Noise in Broadband Optical Sources for Optical Coherence Tomography," IEEE Photonics Technology Letters, 22, 1057–1059, (2010).

[10] Takei, N., Miranda, M., Miyazawa, Y., Kozuma, M. "Simultaneous Suppression of Thermal Phase Noise and Relative Intensity Noise in a Fiber-Optic Gyroscope," IEEE Sensors Journal, 23, 2249–2254, (2023).

[11] Morris, T.A., Zawada, A.N., Garcia, D., Wheeler, J.M., Digonnet, M.J.F., "Optimization of the Angular Random Walk in Laser-Driven Fiber-Optic Gyroscopes," IEEE Sensors Journal, 2205–2212, (2022).

[12] Korsch, H. J., Klumpp, A., Witthaut, D. On two-dimensional Bessel functions. J. Phys. Math. Gen. 2006, 39, 14947

[13] Kuklinski, P., Hague, D. A., "Identities and Properties of Multi-Dimensional Generalized Bessel Functions," arXiv., arXiv:1908.11683, (2021).

[14] Hnatenko, O. S., "Theoretical analysis of the dispersion characteristics of optical elements used in designing fiber lasers," Telecommunications and Radio Engineering (English translation of Elektrosvyaz and Radiotekhnika), 81 (3), 23-31, (2022).

[15] Hnatenko, O. S., "Fiber Laser Based on Electronically Controlled Phase Plates," Journal of Nano- and Electronic Physics, 13 (5), 1-6, (2021).

[16] Gnatenko, A. S., Machekhin, Yu. P., Kurskoy, Yu. S., Obozna, V. P., Vasianovych, A. V., "Ring fiber lasers for telecommunication systems," Telecommunications and Radio Engineering (English translation of Elektrosvyaz and Radiotekhnika), 77 (6), 541-548 (2018).

[17] Machekhin, Yu. P., Kurskoy, Yu. S., Gnatenko, A. S., Tkachenko, V. A. Nanolaser superradiation in information and measuring procedures Telecommunications and Radio Engineering (English translation of Elektrosvyaz and Radiotekhnika), 77 (13), 1179-1186, (2018).

[18] MacHekhin, Yu. P., Kurskoi, Yu. S., Gnatenko, A. S., "Physical and mathematical foundations of measurements in nonlinear dynamic systems," Telecommunications and Radio Engineering (English translation of Elektrosvyaz and Radiotekhnika), 77 (18), 1631-1637 (2018).

[19] Kurskoy, Y. S., Hnatenko, O. S., Afanasieva, O. V., "Precision Synchronization of Chaotic Optical Systems," Journal of Nano- and Electronic Physics, 13 (4), 1-5 (2021).

[20] Zabolotna, N. I., Radchenko, K. O., Tarnovskiy, M. H., "System of Mueller-Jones matrix polarizing mapping of blood plasma films in breast pathology," Proc. SPIE 10407, 1040714 (2017).

[21] Avrunin O. G., Tymkovych M. Y., Saed H. F. I., et al. "Application of 3D printing technologies in building patient-specific training systems for computing planning in rhinology," Information Technology in Medical

Diagnostics II - Proceedings of the International Scientific Internet Conference on Computer Graphics and Image Processing and 48th International Scientific and Practical Conference on Application of Lasers in Medicine and Biology, 7, (2019).
[22] Selivanova K.G., Avrunin O.G., Tymkovych M.Y., Manhora T.V., et al. "3D visualization of human body internal structures surface during stereo-endoscopic operations using computer vision techniques," Przeglad Elektrotechniczny, 9, 30-33, (2021).